Journal of Solid State Chemistry 182 (2009) 1481–1491

Contents lists available at ScienceDirect

Journal of Solid State Chemistry

journal homepage: www.elsevier.com/locate/jssc

Ionic diffusion mastering using crystal-chemistry parameters: τ-$Cu_{1/2}Ag_{1/2}V_2O_5$ structure determination and comparison with refined δ-$Ag_xV_2O_5$ and ε-$Cu_xV_2O_5$ ones

P. Rozier [a,b,*], M. Dollé [a,b], J. Galy [a,b]

[a] Centre d'Elaboration de Matériaux et d'Etudes Structurales-CNRS 29, rue Jeanne Marvig, BP 94347, 31055 Toulouse cedex 4, France
[b] Université de Toulouse, UPS, 118 route de Narbonne, 31062 Toulouse, France

ARTICLE INFO

Article history:
Received 9 February 2009
Received in revised form
19 March 2009
Accepted 20 March 2009
Available online 5 April 2009

Keywords:
Crystal-chemistry
Ionic diffusion
Vanadium oxide
Structure determination

ABSTRACT

τ-$Ag_{1/2}Cu_{1/2}V_2O_5$ compound crystallises in the monoclinic system space group $C2/m$ with cell parameters $a = 11.757(4)$ Å, $b = 3.6942(5)$ Å, $c = 9.463(2)$ Å, and $\beta = 114.62(2)^\circ$. The structure is build up with V_4O_{10} D4 double layer. The silver and copper ions are located in two different oxygenated tunnels. Examination of electronic density maps shows that while the silver ions are located in defined crystallographic sites, the copper ones are fully delocalised over the whole tunnel. Comparison with δ-$Ag_xV_2O_5$ and ε-$Cu_xV_2O_5$ refined structure allows to define crystal chemistry parameters governing the ionic delocalisation and give clues to predict from structural consideration the expected electrical behaviour with the aim to make possible a structural design to enhance guest species reactivity.

1. Introduction

Recent developments in the field of new concepts of lithium reactivity have shown that the basic and well-known criteria allowing to predict that a compound can be a good candidate as active materials for lithium batteries have to be redefined [1]. Especially it was commonly admitted that to be active a compound should present in the charged state empty space which can then be filled by lithium cations during the discharge process. The discovering of both conversion and displacement phenomena indicated that even fully dense a compound can be active as soon as at least one element can be reduced to the metal state and extruded out of the structure. However, the reversibility of such phenomena was at that time identified as poor, preventing for use in batteries [2]. More recently the discovering of combined displacement insertion (CDI) materials shows that in some cases the displacement mechanism can be fully reversible. Firstly evidenced on $Cu_{7/3}V_4O_{11}$ [3], investigation of different compounds selected in systems including Ag or Cu as displaced species and Nb or V as reducible ones allowed to enlighten that the existence, the efficiency and the reversibility of this process is governed by the stability of displaceable cations itself evidenced by a careful examination of its localisation in the structure [4–6]. These results drive to define more precisely the notions of host network and guest species, commonly used in solid state electrochemistry, both of them being enlarged to take into account the efficiency of displacement process. The delocalisation of the cation over several crystallographic sites indicates less bounded specie that can then be considered as mobile and reactive (guest specie) while the localisation on defined sites is the evidence for immobile and unreactive element that have to be included in the definition of the host network.

Crystal chemistry investigations carried out on model compounds have shown that the existence and efficiency of displacement process is related to the existence of a competitive effect between elements to generate, via host network flexibility, their own stable surrounding [7]. The element which presents the less stable surrounding appears delocalised and can be considered as mobile and reactive. The delocalisation is the result of the combination of both host network flexibility parameters and strength of the bond engaged by the guest specie with the host network. The more the strength is, the more the surrounding will be stable. A fully flexible host network (0D or 1D) allows all movement necessary to stabilise any kind of guest leading to unreactive species while 3D network do not present flexibility high enough to accommodate different nature of guest. A 2D network appears to be the best compromise allowing some flexibility to accommodate the different guests but some rigidity to prevent the full stabilisation.

In order to go deeper in the definition of crystal parameters governing the displacement process, we decided to investigate the influence of guest species nature and amount changes while

* Corresponding author. Fax: +33 5 62 25 79 99.
E-mail address: rozier@cemes.fr (P. Rozier).

0022-4596/$ - see front matter © 2009 Elsevier Inc. All rights reserved.
doi:10.1016/j.jssc.2009.03.017

maintaining constant the host network. As Ag and Cu ions are known to be displaceable species and that Ag–V_2O_5 and Cu–V_2O_5 phases present similar structures, we decided to start this investigation on the mixed (Ag and Cu)–V_2O_5 system.

Despite an abundant literature on vanadium oxide based systems, the existence of mixed $(Ag,Cu)_xV_2O_5$ phases are only suggested on the basis of X-ray diffraction patterns collected on powdered samples but without structural details neither than accurate certainties [8]. To settle the number and homogeneity range of the different expected phases, we carried out experiments using an unconventional solid state chemistry route which derive from the Spark Plasma Sintering technique. Initially devoted to fast sintering, this easy to handle technique allows, by a direct control of the nature of reactants and process parameters, to screen in few and short (minutes) experiments a system. The efficiency of this process firstly demonstrated on known (Ag or Cu)–V_2O_5 systems [9] has been used to investigate the mixed (Ag and Cu)–V_2O_5 one leading to evidence the existence of only a phase $(Ag,Cu)_xV_2O_5$ with an homogeneity domain $0<x<0.6$ and a defined compound with a composition close to $Cu_{1/2}Ag_{1/2}V_2O_5$ [10]. Once identified, the understanding of both crystal chemistry parameters governing the formation of these compounds as well as the link with the properties in terms of reactivity implies that a full and deep investigation of their structure is necessary. That can be done only by going back to conventional synthesis routes however focused on compositions rapidly determined by the fast investigation using SPS.

The aim of this paper is to report the crystal chemistry parameters governing the influence of both the nature (Ag or Cu) and the amount of "guest species" on the structural arrangements and their stability. The structure of the mixed $Cu_{1/2}Ag_{1/2}V_2O_5$ is determined and compared to the purely Cu or Ag based homologous. To enhance the accuracy of the comparison and evidenced parameters, single crystal of the latter compounds are prepared and the structure refined.

The similarities and differences are enlightened to settle the crystal chemistry parameters governing the stabilisation of the structures and to predict the behaviour of each of the guest species in terms of both mobility and reactivity.

2. Experimental part

2.1. Synthesis

Powdered samples: $M_xV_2O_5$ samples (M = Ag, Cu or a mixture of them) have been prepared following conventional solid state routes for mixed valence oxides. The reactants, Ag and Cu metal and V_2O_5 are weighed in stoichiometric amounts to reach the desired composition. They are grounded in an agate mortar and the mixture is placed in a quartz tube sealed under vacuum to avoid any risk of oxidation. To prevent any secondary reaction with quartz, a platinum foil isolates the mixture from the tube. The syntheses are performed at 620 °C for 12 h. The products are controlled by means of X-ray diffraction before to be annealed under the same conditions to enhance both homogeneity and crystallinity of the samples.

Single crystal: Powdered samples characterised as single phased materials are placed in a platinum crucible and heated, under vacuum, up to their melting point. The cooling rate is settle to 1 °C/h until a temperature reaching 80% of the melting point. The sample is then cooled down to room temperature following the furnace inertia. In all cases black acicular single crystals are obtained. A part of the preparation is kept for further structural analysis while the rest of the sample is grounded and analysed by XRD. This analysis confirms that the single crystals are representative of the powdered materials and indicate a congruent melting. The experimental pattern is also compared to the one calculated using results of the structure indicating that the selected single crystals are representative of the powdered samples.

2.2. Characterisation

Powder X-ray diffraction: The samples obtained after each heat treatment are controlled by means of powder X-ray diffraction using a Seifert 3000TT diffractometer with monochromatised Cu$K\alpha$ radiation ($\lambda = 1.5418$ Å). X-ray patterns are measured in the 5°–55° 2θ range in a step scan mode with a counting time of 4 s and an angular step width of $0.02° \times 2\theta$.

Single crystal X-ray diffraction: X-ray studies were carried out on a four circles diffractometer Bruker Kappa-CCD (Apex II) working with a Mo$K\alpha$ ($\lambda = 0.7107$ Å) source. Data integration and reduction were carried out using EVALCCD software [11]. SIR 92 [12] was used to solve the structure by direct methods using a F^2 refinement method. The integrated data were refined using SHELXL-97 [13] suite of programs within WIN-GX [14].

3. Results and discussion

3.1. Investigation of $Cu_{1/2}Ag_{1/2}V_2O_5$

3.1.1. Homogeneity range

Fast synthesis experiments using the spark plasma sintering (SPS) techniques have evidenced the absence of a wide homogeneity range around the $Cu_{1/2}Ag_{1/2}V_2O_5$ composition [10]. The use of this technique as a solid state chemistry route being relatively new we decided to validate that using conventional solid state route.

Following chemical processes described in the experimental part, several compositions $Cu_xAg_yV_2O_5$ have been tested in the range $0.6<x+y<1.0$ while checking also the x/y ratio influence

Table 1
Crystal data and structure refinement for τ-$Cu_{1/2}Ag_{1/2}V_2O_5$.

Empirical formula	$Ag_{0.45}Cu_{0.43}V_2O_5$	
Melting temperature (°C)	680	
Formula weight	296.6	
Temperature (K)	293(2)	
Wavelength (Å)	0.71073	
Crystal system	Monoclinic	
Space group	$C2/m$	
Unit cell dimensions	$a = 11.757(4)$ Å	$\alpha = 90°$
	$b = 3.6942(5)$ Å	$\beta = 114.62(2)°$
	$c = 9.463(2)$ Å	$\gamma = 90°$
Volume (Å^3)	373.6(2)	
Z	4	
Density (calculated) (mg/m^3)	4.757	
Absorption coefficient (mm^{-1})	9.56	
F(000)	496	
Crystal size (mm^3)	$0.04 \times 0.1 \times 0.07$	
Theta range for data collection (deg)	5.84–34.99	
Index ranges	$-18 \leqslant h \leqslant 18$, $-5 \leqslant k \leqslant 5$, $-15 \leqslant l \leqslant 15$	
Reflections collected	5033	
Independent reflections	914 [R(int) = 0.1017]	
Completeness to theta = 34.99°	99.0%	
Refinement method	Full-matrix least-squares on F^2	
Data/restraints/parameters	914/0/72	
Goodness-of-fit on F^2	1.094	
Final R indices [$I>2$sigma(I)]	$R1 = 0.0662$, $wR2 = 0.1019$	
R indices (all data)	$R1 = 0.0975$, $wR2 = 0.1093$	
Largest diff. peak and hole	2.515 and −1.463 e Å^{-3}	

($1/3 < x/y < 3/1$). The obtained samples have been characterised using XRD. The comparison of the experimental patterns with those reported in the different databases clearly shows that apart $Cu_{1/2}Ag_{1/2}V_2O_5$ all other compositions lead to mixture including this mixed compound together with purely δ-$Ag_xV_2O_5$ or ε-$Cu_xV_2O_5$ vanadium bronzes. The nature and ratio of the different compounds are in perfect agreement with expected ones confirming the absence of homogeneity range.

3.1.2. $Cu_{1/2}Ag_{1/2}V_2O_5$ structure determination

Several single crystals have been selected and their quality checked. All of them present diffuse scattering lines indicative of complex incommensurable superstructure. However, in light of our previous studies on $Cu_{7/3}V_4O_{11}$ composite structure [15–17], it appears that the determination of the average structure is accurate enough to settle pertinent crystal chemistry parameters to be compared to the one obtained on purely Ag or Cu based compounds.

The cell parameters are determined from the collection of 40 diffraction peaks using the program EvalCCD [11]. The compound crystallises in the monoclinic system with possible space groups *C*2/*m*, *Cm* and *C*2. The most symmetrical one *C*2/*m* is firstly chosen for the structure determination. The heavy V and some of the silver and copper ions are located by direct methods while the oxygen ones and remaining silver and copper ions are located by Fourier difference synthesis. The crystal data and structure refinement parameters are summarised in Table 1.

Two different crystallographic sites are found for the vanadium ions both of them being located in distorted octahedral oxygenated surroundings. The silver cations are described using one main crystallographic site (Ag1) settled in an oxygen trigonal prism. However the presence of residual electronic density that cannot be taken into account by displacement parameters shows some delocalisation of the silver ions around this main site. To describe it, a second position (Ag2) is introduced. The refinement of the occupancy of both sites leads to an overall composition of 0.45 mainly located on the former one. The Fig. 1a shows the oxygenated surrounding of Ag1, considered as the main position. The electronic density map calculated using experimental data (Fig. 1b) confirms the slight delocalisation of the silver cations.

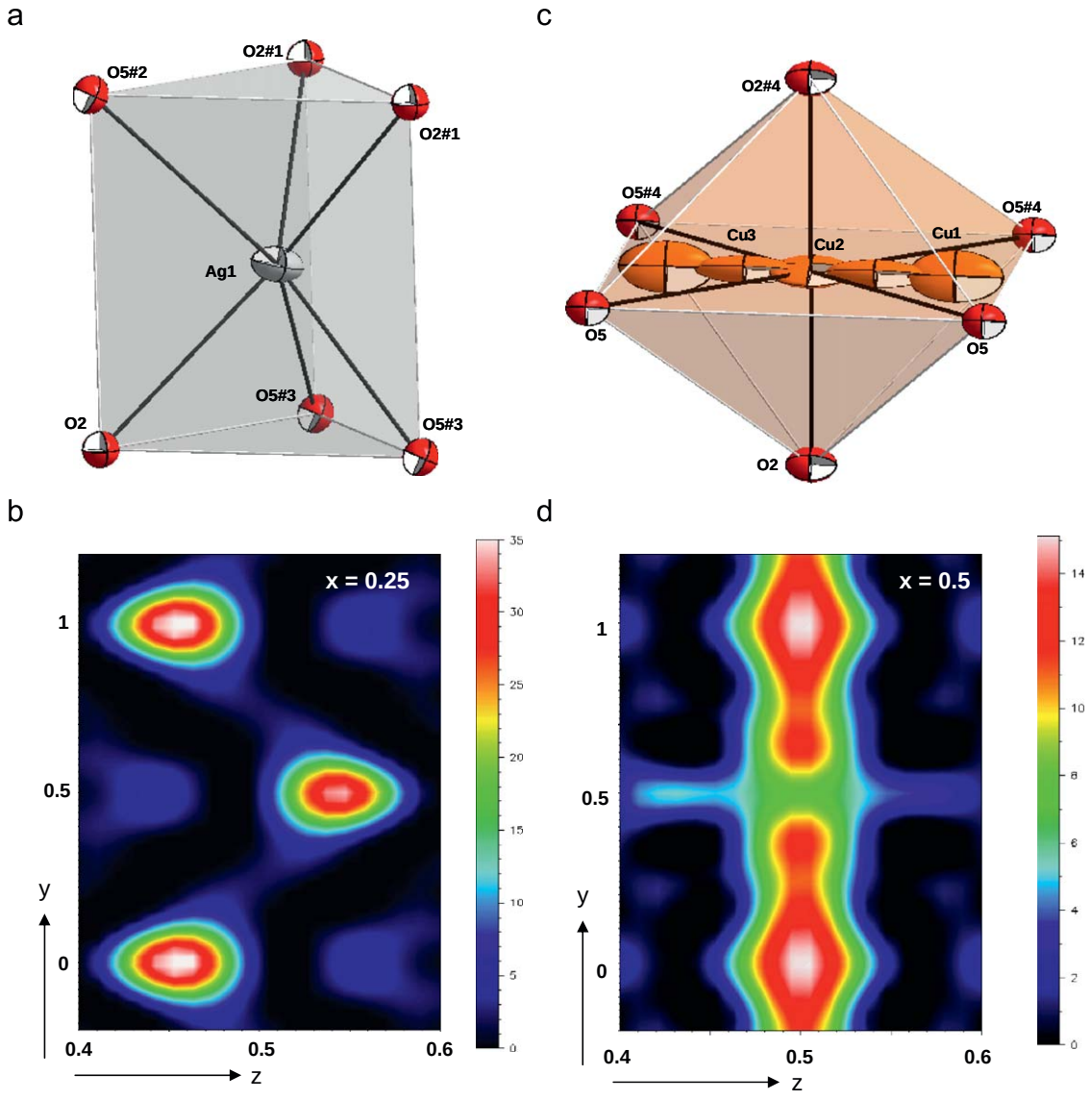

Fig. 1. Silver (a, b) and copper (c, d) surrounding and electronic density map in τ-$Cu_{1/2}Ag_{1/2}V_2O_5$ structure.

The copper ions are even more difficult to localise and should be at the origin of the incommensurate superstructure. The electronic density map calculated using experimental data (Fig. 1d) shows that copper ions can be considered as randomly distributed in a tunnel running along the *b* axis. To describe it, three main contributions are used. They correspond to successive octahedral (Cu2) and tetrahedral (Cu1 and Cu3) oxygenated surroundings (Fig. 1c) almost equally occupied (close to 0.16 for each site). However in each case residual electron densities are found between these main sites. The use of anisotropic displacement parameters does not allow to describe them implying that the definition of extra-crystallographic sites, some of them with

Table 2
Atomic coordinates and equivalent isotropic displacement parameters ($Å^2 \times 10^3$) for τ-$Cu_{1/2}Ag_{1/2}V_2O_5$.

	SOF	*x*	*y*	*z*	*U* (eq)
Ag1	0.289	0.2697(8)	1/2	0.553(1)	24(2)
Ag2	0.081	0.239(1)	0.114(7)	0.462(2)	54(9)
Cu1	0.154	1/2	0.865(5)	1/2	38(6)
Cu2	0.168	1/2	1/2	1/2	34(9)
Cu3	0.189	1/2	0.335(6)	1/2	40(9)
V1		0.2876(1)	1/2	0.1612(1)	6(1)
V2		0.4897(1)	0	0.1650(1)	6(1)
O1		0.1143(5)	1/2	0.1071(6)	9(1)
O2		0.3368(5)	1/2	0.3516(6)	16(1)
O3		0.3007(5)	0	0.1131(6)	7(1)
O4		0.4452(4)	1/2	0.1355(6)	7(1)
O5		0.5610(5)	0	0.3562(6)	14(1)

U (eq) is defined as one-third of the trace of the orthogonalized U^{ij} tensor.

Table 3
Selected inter-atomic distances (Å) for τ-$Cu_{1/2}Ag_{1/2}V_2O_5$.

V1–O2	1.647(6)	V2–O5	1.648(6)
V1–O1	1.883(5)	V2–O1♯5	1.765(5)
2*V1–O3	1.924(2)	2*V2–O4	1.908(2)
V1–O4	1.967(5)	V2–O3	2.067(5)
V1–O3♯4	2.360(5)	V2–O1♯4	2.345(5)
Ag1–O2	2.34(1)	Ag2–O5♯3	2.31(2)
Ag1–O5♯2	2.38(1)	Ag2–O2♯1	2.32(2)
2*Ag1–Ag02	2.60(2)	Ag2–O2	2.34(2)
2*Ag1–O5	2.586(8)	Ag2–O5♯2	2.38(2)
2*Cu1–O5	1.851(7)	2*Cu3–O2	1.945(8)
2*Cu1–O2	2.29(2)	2*Cu3–O5	2.17(2)
4*Cu2–O5	2.567(6)		
2*Cu2–O2	1.847(6)		

Symmetry transformations used to generate equivalent atoms: ♯1 $-x+1/2,-y+1/2,-z+1$, ♯2 $x-1/2,y+1/2,z$, ♯3 $-x+1,-y,-z+1$, ♯4 $-x+1/2,-y+1/2,-z$, ♯5 $x+1/2,y-1/2,z$.

Table 4
Crystal data and structure refinement for δ-$Ag_xV_2O_5$ and ε $Cu_xV_2O_5$.

Empirical formula	$Ag_{0.84}V_2O_5$	$Cu_{0.95}V_2O_5$
Formula weight	289.75	245.42
Temperature (K)	293(2)	293(2)
Wavelength (Å)	0.71073	0.71073
Crystal system	Monoclinic	Monoclinic
Space group	*C*2/*m*	*C*2/*m*
Unit cell dimensions	$a = 11.770(1)$ Å $\alpha = 90°$ $b = 3.6748(2)$ Å $\beta = 90.537(7)°$ $c = 8.7394(8)$ Å $\gamma = 90°$	$a = 11.765(1)$ Å $\alpha = 90°$ $b = 3.6943(2)$ Å $\beta = 111.573(7)°$ $c = 8.9712(8)$ Å $\gamma = 90°$
Volume	377.99(6) $Å^3$	362.61(4) $Å^3$
Z	4	4
Absorption coefficient (mm^{-1})	9.865	8.061
Crystal size (mm^3)	$0.01 \times 0.1 \times 0.01$	$0.01 \times 0.1 \times 0.01$
Theta range for data collection (deg)	4.16–33.85	5.83–32.00
Index ranges	$-18 \leqslant h \leqslant 17$, $-5 \leqslant k \leqslant 5$, $-13 \leqslant l \leqslant 13$	$-17 \leqslant h \leqslant 17$, $-5 \leqslant k \leqslant 5$, $-13 \leqslant l \leqslant 13$
Reflections collected	6427	4307
Independent reflections	831 [R(int) = 0.0289]	711 [R(int) = 0.1010]
Completeness to	theta = 33.85°:96.3%	theta = 32.00°:99.0%
Refinement method	Full-matrix least-squares on F^2	Full-matrix least-squares on F^2
Data/restraints/parameters	831/0/57	711/0/55
Goodness-of-fit on F^2	1.210	1.101
Final *R* indices [$I > 2$sigma(I)]	$R1 = 0.0219$, $wR2 = 0.0546$	$R1 = 0.0630$, $wR2 = 0.1022$
R indices (all data)	$R1 = 0.0237$, $wR2 = 0.0553$	$R1 = 0.0917$, $wR2 = 0.1064$
Largest diff. peak and hole (e $Å^{-3}$)	2.029 and −0.816	1.550 and −1.606

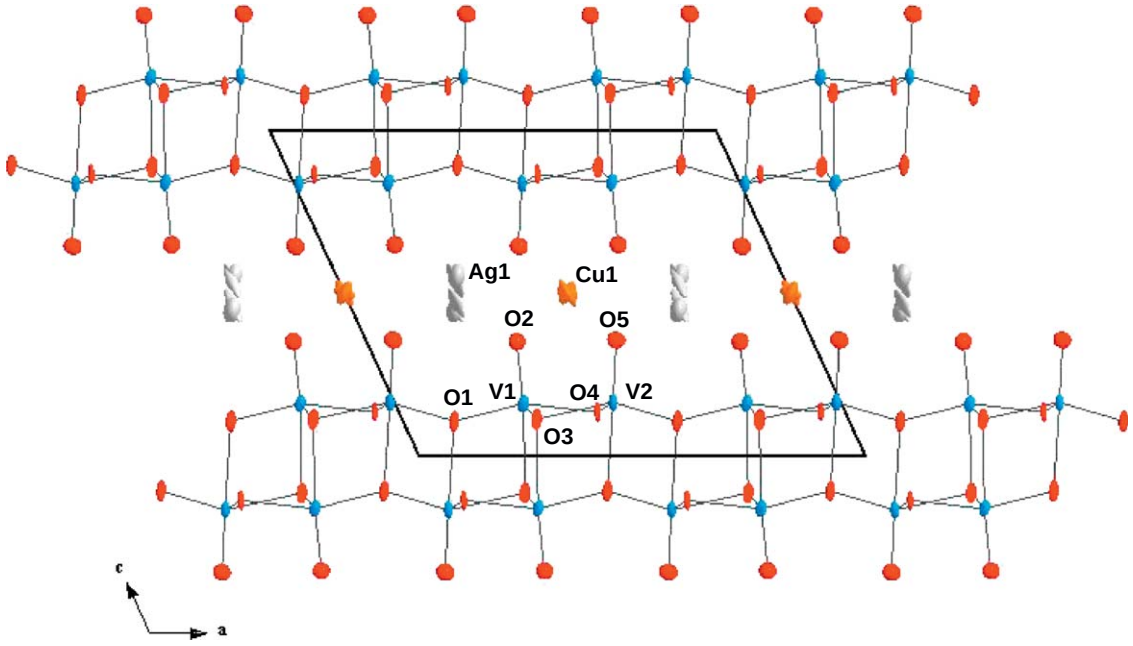

Fig. 2. Projection along [010] of τ-$Cu_{1/2}Ag_{1/2}V_2O_5$ structure.

very low occupancy, is necessary. However that leads to an increase of refined parameters not in agreement with accuracy of structure determination. To limit this effect we decided to describe only the main sites.

Table 5
Atomic coordinates and equivalent isotropic displacement parameters ($Å^2 \times 10^3$) for δ-$Ag_xV_2O_5$.

	SOF	x	y	z	U (eq)
Ag01	0.64	0.6222(1)	1/2	0.5227(2)	20(1)
Ag02	0.20	0.578(2)	1/2	0.5336(4)	57(2)
V01		0.0658(1)	1/2	0.1650(1)	6(1)
V02		0.2690(1)	0	0.1615(1)	7(1)
O01		−0.0781(2)	1/2	0.1021(2)	10(1)
O02		0.0549(2)	1/2	0.3524(2)	15(1)
O03		0.1009(2)	0	0.1388(2)	9(1)
O04		0.2384(2)	1/2	0.1147(2)	9(1)
O05		0.2878(2)	0	0.3476(2)	15(1)

U (eq) is defined as one-third of the trace of the orthogonalized U^{ij} tensor.

Table 6
Selected inter-atomic distances (Å) for δ-$Ag_xV_2O_5$.

2*Ag01–O05	2.400(2)	Ag02–O02♯4	2.439(3)
Ag01–O05♯3	2.489(3)	Ag02–O02♯3	2.439(3)
2*Ag01–O02	2.489(2)		
2*Ag01–O2	2.993(4)		
V01–O02	1.644(2)	V02–O05	1.639(2)
V01–O01	1.776(2)	V02–O01♯4	1.878(2)
2*V01–O03	1.8975(5)	2*V02–O04	1.9159(6)
V01–O04	2.082(2)	V02–O03	1.986(2)
V01-O01♯6	2.341(2)	V02–O04♯8	2.415(2)

Symmetry transformations used to generate equivalent atoms: ♯1 $-x+1,-y+1,-z+1$, ♯2 $-x+1,-y,-z+1$, ♯3 $x+1/2,y+1/2,z$, ♯4 $x+1/2,y-1/2,z$, ♯5 $x,y+1,z$, ♯6 $-x,-y+1,-z$, ♯7 $x,y-1,z$, ♯8 $-x+1/2,-y+1/2,-z$, ♯9 $x-1/2,y+1/2,z$, ♯10 $x-1/2,y-1/2,z$.

Final atomic coordinates and isotropic thermal parameters are given in Table 2 while a selection of inter-atomic bond lengths is gathered in Table 3.

The projection of the structure is reported in Fig. 2. The VO_6 octahedra share edges to form the D4 type layer [18] developed in the (001) plane. The layers are stacked along the [001] direction in such a way that they define two kinds of tunnel. Each type of tunnel is filled with only one of the guest species leading to an ordered occupancy with alternatively copper or silver ions along the [100] direction. The copper ions are almost fully delocalised along their tunnel with however three main sites while the silver ions are slightly delocalised around their main site.

The refinement of the occupancy of the different positions leads to a formula $Ag_{0.45}Cu_{0.43}V_2O_5$ in agreement with the expected and reported ones. However one has to note that as not all of the electron density can be described, the effective composition can be somewhat around the announced one.

3.1.3. *Binary $M_xV_2O_5$ (M = Ag or Cu) structure refinement*

To go deeper in the understanding of the influence of the simultaneous presence of copper and silver ions we decided to compare the structural arrangement determined in the case of mixed $Ag_{1/2}Cu_{1/2}V_2O_5$ compound to the already investigated $Ag_xV_2O_5$ and $Cu_xV_2O_5$ single guest species ones [19–25].

In both Ag–V_2O_5 and Cu–V_2O_5 systems mainly two domains are evidenced. The first one obtained for low guest species content ($x<0.6$) corresponds to the well-known β-$M_xV_2O_5$ structure type common to several M based systems. The second domain ($0.7<x<0.9$ range) corresponds to two structures δ-$Ag_xV_2O_5$ and ε-$Cu_xV_2O_5$ built up using the same D4-type layers but with different stacking sequence. This difference leads to stabilise different oxygenated surroundings for the Ag and Cu species: a monocapped trigonal prism for the former and octahedral or square planar for the latter one.

Even though the copper based structure has been refined recently, no refinement of the silver based one has been carried out since its determination in 1965 by Anderson. In order to be

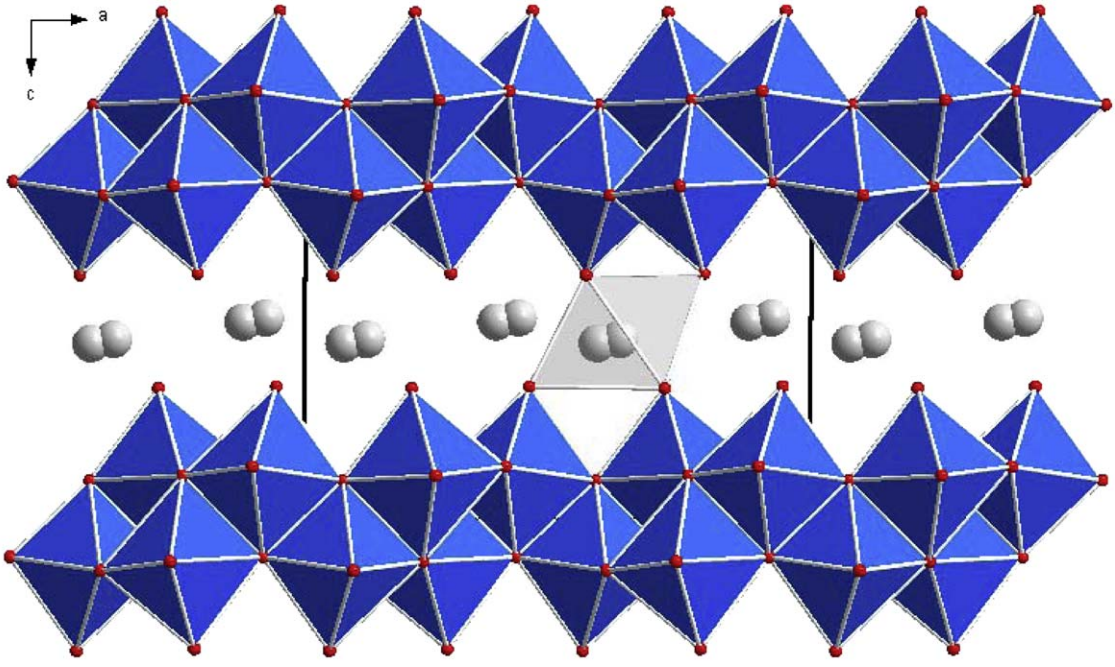

Fig. 3. Projection along [010] of δ-$Ag_xV_2O_5$ structure.

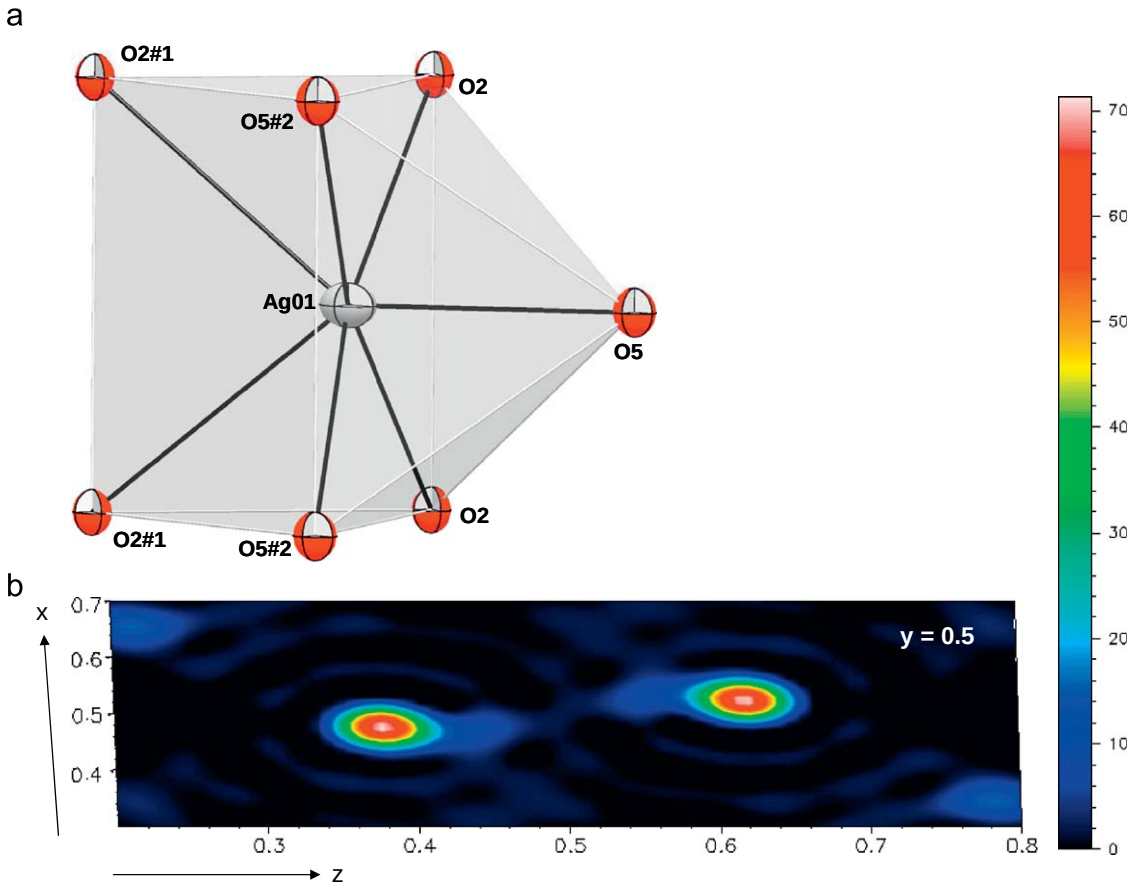

Fig. 4. Silver surrounding (a) and electronic density maps (b) in δ-$Ag_xV_2O_5$ structure.

able to make accurate comparison of the influence of the presence of Ag or Cu or a mixture of both cations on the structural arrangement we decided to re-investigate both δ-$Ag_xV_2O_5$ and ε-$Cu_xV_2O_5$ structures with a special attention paid on the determination of the guest Ag and Cu ions locations.

The synthesis, crystal growth and single crystal analysis follow the same process than previously described. The parameters used for data collection and refinement are reported in Table 4. As the structures of the δ-$Ag_xV_2O_5$ and ε-$Cu_xV_2O_5$ have yet been reported, we only focus on the refinement of the Ag or Cu ions location and to the structural parameters suitable for accurate comparison with the mixed $Cu_{1/2}Ag_{1/2}V_2O_5$ compound.

3.1.4. δ-$Ag_xV_2O_5$ structure refinement

δ-$Ag_xV_2O_5$ crystallises in the monoclinic system with space group $C2/m$. Final atomic coordinates and isotropic thermal parameters are given in Table 5 while a selection of inter-atomic bond lengths is gathered in Table 6.

The vanadium elements are located in distorted VO_6 octahedra sharing edges to form the D4 layers developed in the (001) plane and stacked along the [001] direction (Fig. 3). The stacking sequence generates one kind of oxygenated tunnels in which the silver cations are located. They are described using one crystallographic site (Ag01) located out of $2/m$ symmetry element but still in the mirror plane leading to distorted monocapped trigonal prism oxygenated surrounding (Fig. 4a). However the presence of residual electron density that cannot be taken into account by displacement parameters shows some delocalisation of the silver ions around this main site. The electronic density map

Table 7
Atomic coordinates and equivalent isotropic displacement parameters ($Å^2 \times 10^3$) for ε $Cu_xV_2O_5$.

	SOF	x	y	z	U (eq)
Cu01	0.99	1/2	1/2	1/2	25(1)
Cu02	0.44	1/4	1/4	1/2	32(1)
V01		0.2802(1)	1/2	0.1636(2)	8(1)
V02		0.4824(1)	0	0.1685(2)	7(1)
O01		0.1084(5)	1/2	0.1096(8)	12(1)
O02		0.3219(6)	1/2	0.3655(8)	14(1)
O03		0.2959(5)	0	0.1134(8)	10(1)
O04		0.4402(5)	1/2	0.1420(8)	9(1)
O05		0.5449(6)	0	0.3663(8)	16(2)

U (eq) is defined as one third of the trace of the orthogonalized U^{ij} tensor.

Table 8
Selected inter-atomic distances (Å) for ε $Cu_xV_2O_5$.

2*Cu01–O02	1.997(6)	2*Cu02–O02	1.943(6)
4*Cu01–O05	2.365(4)	2*Cu02–O05	2.446(5)
V01–O02	1.693(7)	V02–O05	1.653(7)
V01–O01	1.898(6)	V02–O01♯8	1.747(6)
2*V01–O03	1.926(2)	2*V02–O04	1.905(2)
V01–O04	1.962(6)	V02–O03	2.065(6)
V01–O03♯7	2.312(7)	V02–O01♯7	2.324(7)

Symmetry transformations used to generate equivalent atoms: ♯1 $-x+1,-y+1,-z+1$, ♯2 $-x+1,-y,-z+1$, ♯3 $x,y+1,z$, ♯4 $-x+1/2,y+1/2,-z+1$, ♯5 $-x+1/2,y-1/2,-z+1$, ♯6 $-x+1/2,-y+1/2,-z+1$, ♯7 $-x+1/2,-y+1/2,-zv$, ♯8 $x+1/2,y-1/2,z$, ♯9 $x,y-1,z$, ♯10 $x-1/2,y+1/2,z$.

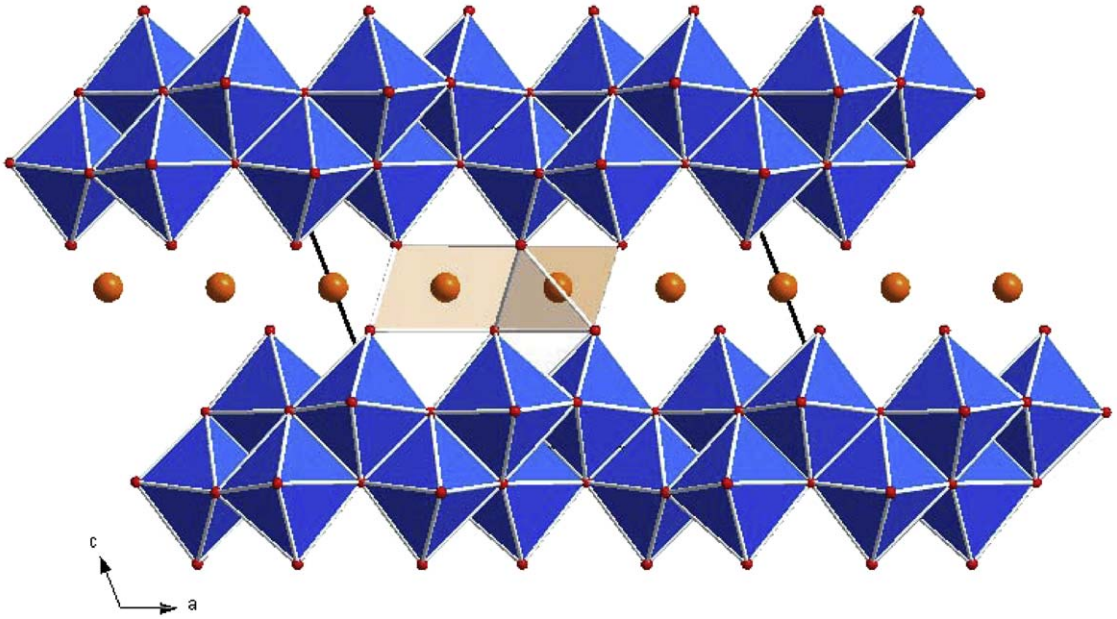

Fig. 5. Projection along [010] of ε-$Cu_xV_2O_5$ structure.

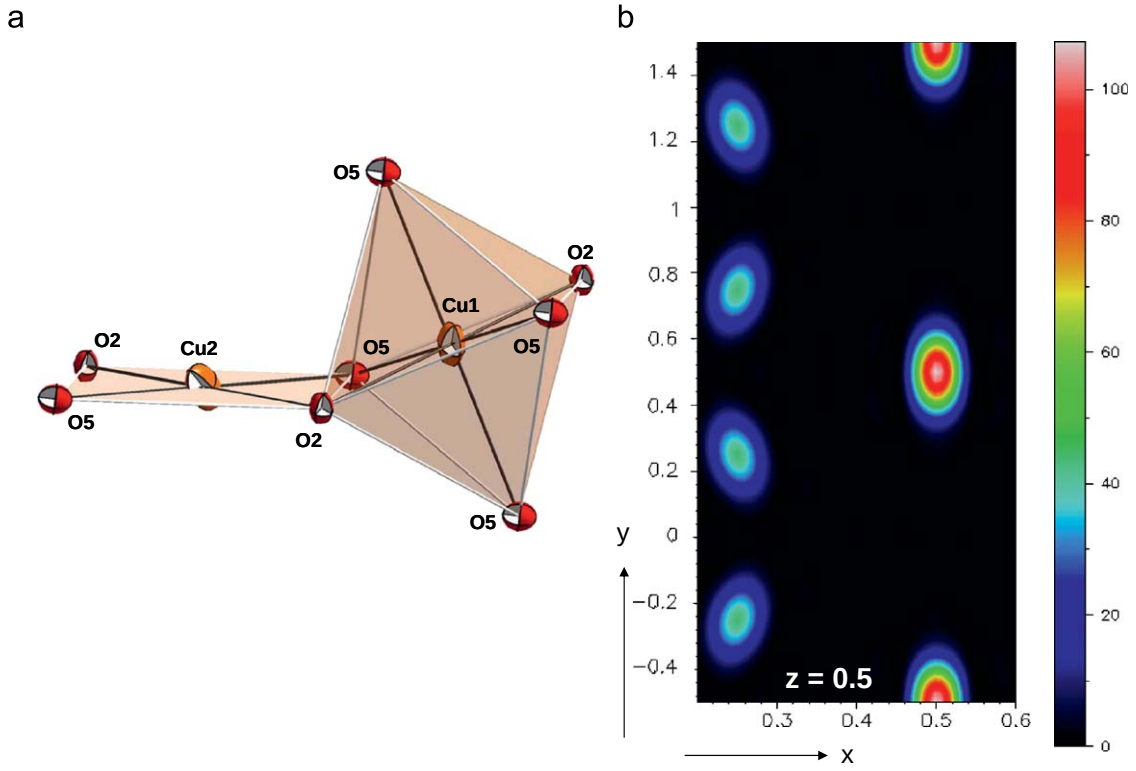

Fig. 6. Copper surrounding (a) and electronic density maps (b) in ε-$Cu_xV_2O_5$ structure.

reported in Fig. 4b confirms the disordered occupancy showing however that it cannot be considered as a full delocalisation of the silver cations in the tunnel. The addition of an extra site (Ag02) very close to the main one (dAg01–Ag02 = 0.532 Å) with low but reasonable occupancy (0.2) complete the description. The refinement of the occupancies leads to the formula $Ag_{0.84}V_2O_5$ while, from structural consideration, the upper limit of the δ $Ag_xV_2O_5$ phase can be settle to $x = 1$ for a full occupancy of the tunnel with Ag ions.

3.1.5. ε-$Cu_xV_2O_5$ structure refinement

ε-$Cu_xV_2O_5$ crystallises in the monoclinic system with space group *C2/m*. Final atomic coordinates and isotropic thermal parameters are given in Table 7 while a selection of inter-atomic bond lengths is gathered in Table 8.

The vanadium elements are located in distorted VO_6 octahedra sharing edges to form the D4 layers developed in the (001) plane and stacked along the [001] direction (Fig. 5). The stacking sequence generates two different oxygenated tunnels leading

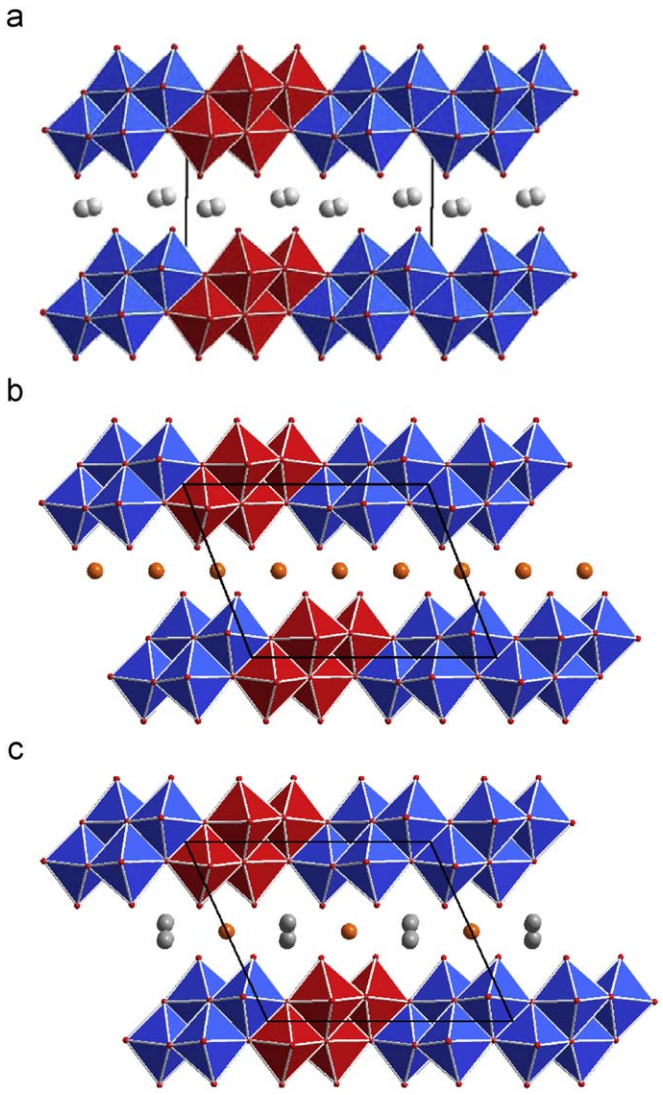

Fig. 7. D4 layer stacking sequence comparison between (a) δ-$Ag_xV_2O_5$; (b) ε-$Cu_xV_2O_5$ and (c) $Cu_{1/2}Ag_{1/2}V_2O_5$ structures.

to two different crystallographic sites for the copper ions Cu01 and Cu02 which correspond to square planar and octahedral surroundings respectively (Fig. 6a). They are located, respectively, on 2/*m* symmetry element (2*c*) and inversion centre (4*f*). The electron density distribution (Fig. 6b) being well described with the use of anisotropic displacement parameters confirms that the copper ions are located in these main sites, Cu01 presents a reverse Jahn–Teller distortion with four large Cu–O distances in the basal plane (2.365(4) Å) and two short apical ones (1.997(6) Å). Cu02 is located in a distorted square planar oxygenated surrounding with two short (1.943(6) Å) and two large (2.446(5) Å) Cu–O distances. The refinement of the site occupancy factor shows that Cu01 is almost fully occupied while for Cu02 the refinement converges to 0.44 close to the maximal expected value (0.5) due to short Cu02–Cu02 distance (1.847 Å) generated by the symmetry. The refined occupancies lead to the formula $Cu_{0.95}V_2O_5$ while, from structural consideration, the upper limit of the ε $Cu_xV_2O_5$ phase can be settle, as for silver based one, to $x = 1$. However one has to note that despite the same limit it corresponds to the full occupancy of the Cu01 site and half occupancy of the Cu02 one instead of full occupancy of the unique silver site.

3.1.6. Structure comparison: determination of the influence of the guest species

As first evidence, one can note that for a given amount of cationic species, the same kind of VO network is formed whatever the nature of the cationic specie. For $0.7 < x < 1$, $M_xV_2O_5$ phases present the same D4 double layer for *M* being silver, copper or a mixture of both of them. This layer does not seem affected by the nature of the cationic species as equivalent distribution of V–O inter-atomic distances (1.65–2.35 Å) is observed. Developed in the (001) plane, the dimensions of D4 layer are given by **a** and **b** cell parameters. They are found almost identical in the three structures confirming that the nature of *M* species does not affect the general organisation of the layers themselves.

The main difference between the compounds is related to the way the layers are stacked which can be identified by the evolution of the monoclinic angle. This can be assigned to the fact that the layers are held together via *M*–O bonds (*M* = Ag or Cu) strongly dependant on the nature of *M* both in terms of *M*–O distances and design of suitable surroundings.

For *M* = Ag, the monoclinic angle is close to 90° and can be considered as an almost perfect alignment of the different D4 layers (Fig. 7a). It drives to design a unique monocapped trigonal prism surrounding suitable for all the silver cations.

For *M* = Cu, the monoclinic angle close to 111° can be interpreted as a 3.3 Å length gliding of the layer along the [100] direction (Fig. 7b). This length is almost equal to one VO_6 octahedra width (average value 3.8 Å) leading to align opposite building units of the D4 layers. This is induced by the necessary design of two independent and different surroundings (square planar and octahedral) suitable for copper ions.

In addition to this gliding, the presence of silver or copper induces also a difference in the interlayer distance decreasing from 2.60 Å for δ-$Ag_xV_2O_5$ down to 2.23 Å for ε-$Cu_xV_2O_5$. Related to the respective size of silver (1.3 Å) and copper (0.8 Å) ions it also explains the evolution of the cell volume which decreases from 378 $Å^3$ down to 363 $Å^3$.

As evidenced, the use of silver or copper cations leads to different stacking sequences of the same D4 layers in agreement with the formation of the different suitable surroundings. One can expect due to the large difference between ending members that a solid solution between them would not be easily stabilised. Therefore, the formation of a mixed compound including both silver and copper cations and built up with the same D4 layers comes as a surprise.

For this mixed compound, the monoclinic angle (114°) is close to that of copper based phase. On this basis, one can suggest that copper ions would govern the gliding of the D4 layers. The evaluation of the interlayer space leads to a value 2.44 Å higher than in ε-$Cu_xV_2O_5$ which is in agreement with the presence of large silver ions but lower than in δ-$Ag_xV_2O_5$. This intermediate value seems to indicate that silver ions have no main effect and would only fill remaining empty sites.

However, a careful examination of the crystallographic parameters shows that the gliding length observed in the mixed compound (3.9 Å) is slightly higher than in copper based phase (3.3 Å). Almost equal to one VO_6 octahedron width (3.8 Å) it leads to a perfect alignment of opposite D4 layer building unit (Fig. 7c). This increased gliding induces the possibility to form an oxygenated trigonal prism suitable for silver ion while maintaining the octahedral surrounding of copper ions. From this second evidence the preponderant role of copper versus silver on the structure design is not so clear than previously described. Despite a stacking sequence and interlayer space close to the one of ε-$Cu_xV_2O_5$ phase, the existence of sites suitable for both Cu and Ag ions prevent for a direct conclusion on the influence of each of

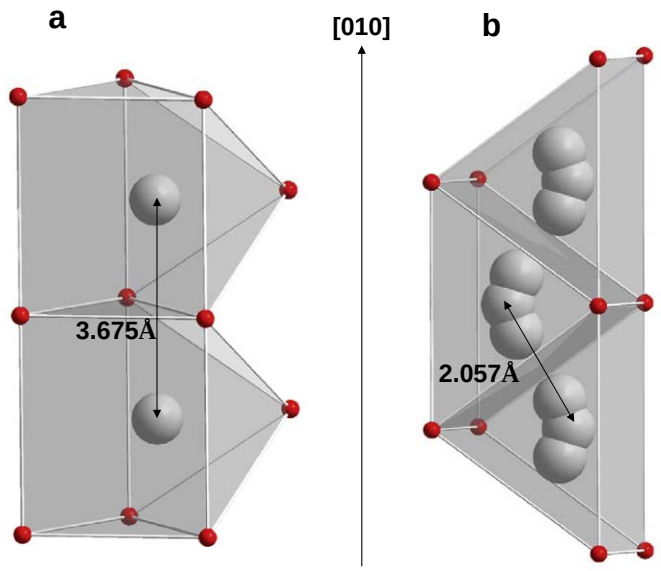

Fig. 8. Silver site evolution in (a) δ-$Ag_xV_2O_5$ and (b) τ-$Cu_{1/2}Ag_{1/2}V_2O_5$ structures.

these specie on the structure showing the need for a careful examination of surrounding evolutions.

3.1.7. Silver based surrounding evolution

The comparison of surroundings determined in δ-$Ag_xV_2O_5$ and in the mixed compound allows exhibiting two differences. The first one, related to the shape of the surrounding, indicates the loss of the seventh capping oxygen in the mixed compound compared to δ-$Ag_xV_2O_5$. It corresponds to a decrease of the coordination number from 7 to 6 associated, as depicted in Fig. 8, to a displacement of silver ion from a rectangular face toward the centre of the trigonal prism. The second difference is related to the orientation and connection way of the surroundings. In the mixed compound the polyhedron appears rotated, the triangular face being parallel to the (010) plane, compared to perpendicular in δ-$Ag_xV_2O_5$. This rotation modifies the connection, along the [010] direction, between polyhedra from triangular face sharing in the latter structure to rectangular face sharing in the former one (Fig. 8). The combination of both silver displacement toward the centre of the prism and the purely rectangular face sharing induces a decrease in the Ag–Ag distance from 3.67 Å in δ-$Ag_xV_2O_5$ structure to 2.06 Å in the mixed compound. Too short for an Ag–Ag inter-atomic distance, it implies that only one every two sites can be occupied in agreement with the experimentally refined value (0.45).

3.1.8. Copper based surrounding evolution

The evolution of the copper surrounding is easily identified due to the similarity of the stacking sequence of the D4 layers in both the starting ε-$Cu_xV_2O_5$ phase and mixed compound. Among the two different sites in the former phase only the octahedral one is kept in the latter one. The slight evolution of the interlayer distance allows maintaining the octahedral shape of the surrounding with however changes in the O–O inter-atomic distances. The most important evolution is evidenced by the shortest O5–O5 distance related to the shortest tunnel width (Fig. 9) which increases from 2.96 Å in ε-$Cu_xV_2O_5$ phase up to 3.57 Å in the mixed compound. The typical reverse Jahn teller distortion of the CuO_6 octahedron is then amplified in the mixed compound as evidenced by the decrease of the two shorts Cu–O distances (2.00 Å down to 1.85 Å) and the increase of the four large ones (2.37 Å up to 2.57 Å). These changes however do not modify the

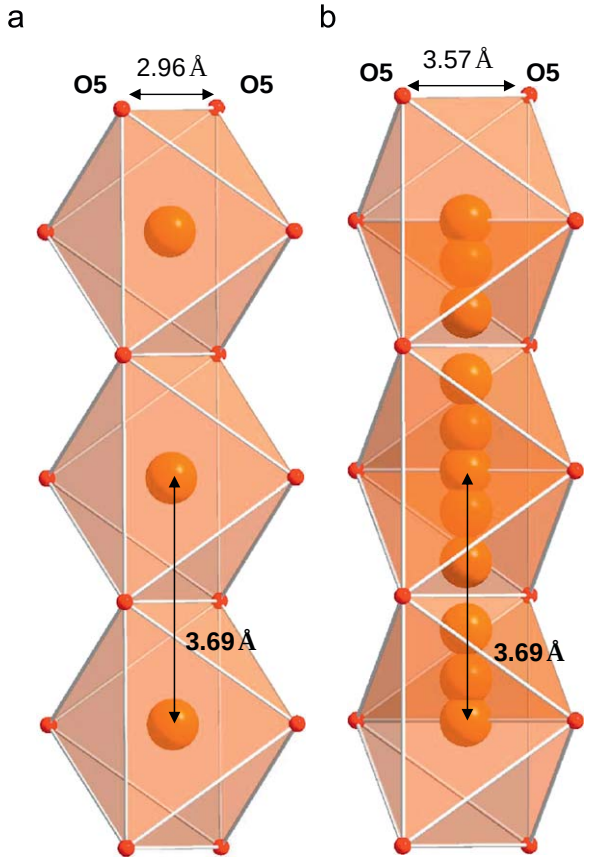

Fig. 9. Copper site evolution in (a) ε-$Cu_xV_2O_5$ and (b) τ-$Cu_{1/2}Ag_{1/2}V_2O_5$ structures.

Cu–Cu inter-atomic distance allowing this site to be fully occupied.

While presenting the same accessible surrounding, the most evident change concerns the localisation of the copper ions themselves. Localised in well-defined sites in the $Cu_xV_2O_5$ phase (Fig. 6b), they are found almost fully delocalised along the oxygenated tunnel in the mixed compound (Fig. 1d).

3.1.9. Interdependent influence of silver and copper

Once compared the surrounding evolution, mainly related to the evolution of the D4 layers stacking sequence, of each of intercalated ions, we decided to determine the effect of the coexistence of two different species in adjacent oxygenated surrounding i.e. to study the effect of the presence of copper ions on the silver location and *vice versa*.

As ε-$Cu_xV_2O_5$ and the mixed compound presenting similar stacking sequence, the formation of the mixed compound can be described as the silver to copper substitution on $Cu_xV_2O_5$ structure. In the ε-$Cu_xV_2O_5$ structure the regular distribution of both copper ions leads to stabilise two sites for copper. The comparison of the inter-atomic Cu–Cu distances (Fig. 10a) indicates that while the Cu01 octahedral site can be fully occupied (Cu01–Cu01 = 3.69 Å) the Cu02 square planar one can only be half occupied (Cu02–Cu02 (1.85 Å)). Despite this half occupancy, the Cu02 ions are randomly distributed over the equivalent positions showing that the Cu01–Cu02 distance (3.08 Å) is high enough to minimise the cationic repulsive effect. The examination of the electron density map (Fig. 6b) shows that the different copper ions are located in well-defined sites indicating that for this composition equilibrium is reached

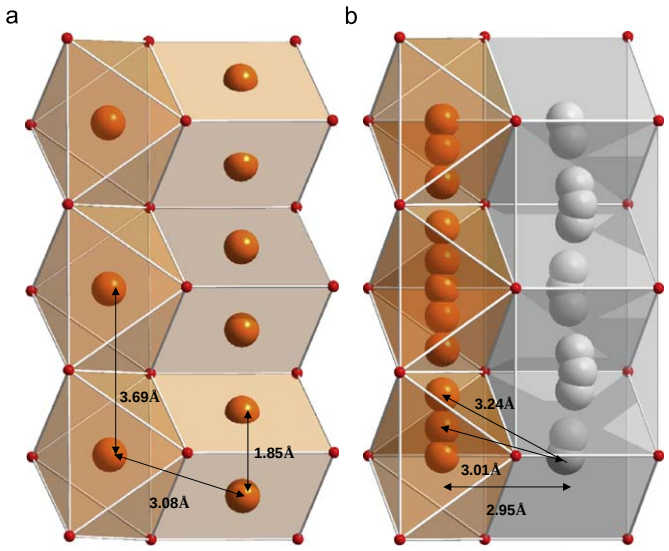

Fig. 10. Site connection in (a) ε-$Cu_xV_2O_5$ and (b) τ-$Cu_{1/2}Ag_{1/2}V_2O_5$ structures.

leading to the structure stabilisation. Assuming that the formation mechanism of the mixed compound results from the substitution of silver to copper in ε-$Cu_xV_2O_5$, the first evidence is that it occurs only on the copper located in square planar surrounding (Cu02) of the pristine phase. The comparison of Cu02 location in ε-$Cu_xV_2O_5$ to Ag1 location in the mixed compound can then be considered as the trace of the crystallographic site evolution during the substitution. To enlighten such evolution, both starting and final positions are described using the same trigonal prism oxygenated surrounding. The substitution of silver to copper can then be interpreted as the displacement along the [010] direction of the site from the centre of the face (copper location) toward the centre of the trigonal prism (silver location). This movement induces the shortening of the Cu1–M distance (from 3.08 Å with $M = Cu02$ to 2.95 Å with $M = Ag1$) leading to cationic repulsive effect high enough to push away the remaining copper ions along [010] direction from the centre (Cu2) of the octahedron toward the tetrahedral (Cu3 site) and further almost linear (Cu1 site) surroundings as determined in the $Ag_{1/2}Cu_{1/2}V_2O_5$ mixed compound. This leads to an increase of the inter-atomic Cu–Ag distance (3.01 and 3.24 Å, respectively) decreasing the repulsive effect. However, this movement implies also that the inter-atomic distance between these new copper positions and the next silver site decreases inducing an increase of the repulsive effect. These competitive effects imply that no stable position can be determined driving to the delocalisation of the copper ions along the tunnel. This fact is confirmed by the electronic density map showing the copper ions fully delocalised while the silver ones are almost localised in the centre of their prismatic sites (Fig. 1).

However, combining both ions localisation and partial occupancy of the silver site an equilibrated configuration can be determined. It corresponds to an ordered localisation of the silver ions one every two sites along the [010] direction. In such a case both octahedral site for copper and prismatic one for silver could be simultaneously occupied while maintaining Cu–Ag distance high enough (3.522 Å) to minimise the repulsive effect and stabilise the structure.

Despite stable, this configuration is not adopted, at least at ambient temperature, leading to random occupancy of localised silver site, itself responsible for copper delocalisation. This specific distribution can be the evidence of the independence of silver and copper locations which should drive to the existence of a two part composite structure. One part would be constituted with both VO network and Ag ions combined in a mixed host network, while the second part would be associated to the copper ions which appear mobile i.e. acting as guest specie.

4. Conclusion

To determine structural parameters governing the stabilisation of a peculiar atomic arrangement as well as its consequences on the reactivity, three different compounds were investigated namely δ-$Ag_xV_2O_5$, ε-$Cu_xV_2O_5$ and τ-$Cu_{1/2}Ag_{1/2}V_2O_5$. They present the same structure type based on the stacking of VO D4 double layers and differ by the stacking sequence as well as the distribution of the cation in the interlayer space.

The careful determination of parameters allows us to settle the origin for both similarities and differences and to relate then to the nature and amount of guest species.

The formation of D4 type layer is related to the amount of guest species whatever its nature (Ag, Cu or a mixture of them). The nature of the guest species via the *M*–O bonds engaged with the layers governs the stacking sequence in such a way that inserted species tend to align host network layers in order to generate their own stable oxygenated surrounding. Easily done in the case where only one type of guest specie is used, that leads to localisation of inserted ions in well-defined crystallographic sites that can be of different shapes and partially occupied to encounter for cationic–cationic repulsive effects. For example the ε-$Cu_xV_2O_5$ structure presents two different surroundings for copper, one octahedral the other one square planar, without any evidence of delocalisation of the different ions showing the stability of the resulting structure.

Using a mixture of guest species, competitive effects occur. The mixed τ-$Cu_{1/2}Ag_{1/2}V_2O_5$ compound presents a stacking sequence close to that of ε-CuV_2O_5 phase indicating that the copper should be the main driver of the structural arrangement. However, going deeper in the structure, one can evidence a full delocalisation of the copper ions along their tunnel while the silver ones remain almost localised on well-defined sites indicating that in fact silver ions are the main drivers of the structural arrangement. Moreover, a stable organisation of the occupancy of the different sites can be proposed driving to both suitable surrounding for the different species and minimisation of cationic–cationic repulsive effect but at that time no reason can be proposed to explain why it does not occur.

Acknowledgments

The Centre National de la Recherche Scientifique (France) is gratefully acknowledged for its financial support. We wish to thank O. Szajwaj for his help in data collection for X-ray diffraction on single crystal measurements.

References

[1] J.M. Tarascon, S. Gougeon, M. Morcrette, S. Laruelle, P. Rozier, Ph. Poizot, C.R. Chimie 8 (2005) 9–15.
[2] K.D. Kepler, J.T. Vaughey, M.M. Thackeray, Electrochem. Solid State Lett. 2 (1999) 307.
[3] M. Morcrette, P. Rozier, L. Dupont, E. Mugnier, L. Sannier, J. Galy, J.M. Tarascon, Nat. Mater. 2 (2003) 755–761.
[4] M. Morcrette, P. Rozier, H. Vezin, F. Chevallier, L. Laffont, P. Poizot, J.M. Tarascon, Chem. Mater. 17 (2) (2005) 418–426.
[5] P. Rozier, M. Morcrette, P. Martin, L. Laffont, J.M. Tarascon, Chem. Mater. 17 (5) (2005) 984–991.

[6] P. Poizot, F. Chevallier, L. Laffont, M. Morcrette, P. Rozier, J.M. Tarascon, Electrochem. Solid State Lett. 8 (4) (2005) A184–A187.
[7] P. Rozier, M. Morcrette, O. Szajwaj, V. Bodenez, M. Dolle, C. Surcin, L. Dupont, J.M. Tarascon, Israel J. Chem. 48 (3–4) (2008) 235–250.
[8] V.L. Volkov, B.G. Golovkin, Russ. J. Inorg. Chem. 33 (1988) 1043–1044.
[9] J. Galy, M. Dollé, T. Hungria, P. Rozier, J.-P. Monchoux, Solid State Sci. 10 (2008) 976–981.
[10] J.P. Monchoux, M. Dollé, P. Rozier, J. Jaud, J. Galy, submitted.
[11] Bruker, Collect and EvalCCD, B.A. Inc. (Ed.), Madison, Wisconsin, 2002.
[12] A. Altomare, J. Appl. Crystallogr. 27 (3) (1994) 435.
[13] G.M. Sheldrick, SHELX-97 a program for crystal structure refinement, 1997.
[14] L.J. Farrugia, J. Appl. Crystallogr. 32 (1999) 837.
[15] P. Rozier, C. Satto, J. Galy, Solid State Sci. 2 (6) (2000) 595–606.
[16] R. Withers, P. Rozier, Z. Kristallogr. 215 (2000) 688–692.
[17] P. Rozier, S. Lidin, J. Solid State Chem. 172 (2003) 319–326.
[18] J. Galy, J. Solid State Chem. 100 (1992) 209–245.
[19] A. Casalot, A. Deschanvres, P. Hagenmuller, B. Raveau, Bull. Soc. Chim. Fr. XC (1965) 1730–1731.
[20] J. Galy, D. Lavaud, A. Casalot, P. Hagenmuller, J. Solid State Chem. 2 (1970) 531–543.
[21] J.M. Savariault, E. Déramond, J. Galy, Z. Kristallogr. 209 (1994) 405–412.
[22] A. Casalot, M. Pouchard, Bull. Soc. Chim. Fr. (1967) 3817–3820.
[23] S. Andersson, Acta Chem. Scand. 19 (1965) 1265–1369.
[24] S. Andersson, Acta Chem. Scand. 19 (1965) 1371–1375.
[25] E. Déramond, J.-M. Savariault, J. Galy, Acta Cryst. C 50 (1994) 164–166.